Bol. Soc. Paran. Mat.
©SPM – E-ISSN-2175-1188
SPM: www.spm.uem.br/bspm

(3s.) **v. 2026 (44) 7** : 1–17.
ISSN-0037-8712
doi:10.5269/bspm.82330

Geometric Methods in Variable-Mass Dynamics with Darboux-Frame

A. Elsharkawy[1], H. K. Elsayied[1], M. E. Desouky[2] and C. Cesarano[3]

ABSTRACT: This study bridges classical mechanics and differential geometry by providing a comprehensive geometric analysis of momentum, force, and their higher-order derivatives for particles moving along space curves. Focusing on both constant-mass and variable-mass systems, we develop a unified theoretical framework using the Frenet and Darboux frames. The core contribution is the resolution of the force derivative, or *yank*, into its intrinsic geometric components, extending Siacci's classical theorem and recent advancements to include this underexplored quantity. We derive formulations for the radial decomposition of yank in the osculating and rectifying planes, offering insights into the transient dynamics of mechanical systems. The theoretical model is applied to specific trajectories, including slant helices, to demonstrate its utility in predicting the behavior of variable-mass systems.

Key Words: Frenet frame, Darboux frame, acceleration, jerk, Siacci's theorem, momentum, force, yank, space curves.

Contents

1. Introduction

Since Newton first formulated his laws of motion, the investigation of dynamic systems has been of prime importance in physical science. Classical mechanics provides the fundamental framework for predicting the behavior of physical bodies under the action of external forces, with Newton's second law serving as its foundational principle. Under this, the time rate of change of a body's momentum equals the net force acting on it, which reduces to the well-known acceleration relationship in the case of constant mass. Most physical systems like rockets, planets, and other mass-flow systems deviate from this theoretical framework because of their time-varying mass nature. Newton's second law is then in need of close adaptation to address mass variation, demanding more careful investigation into the creation of forces and its higher-order derivatives.

The significance of variable forces is especially evident in systems with changing forces in motion. For example, in flight through the atmosphere, rockets continuously lose mass through propellant burn, requiring constant thrust adjustment to maintain acceleration profiles [27]. In astrodynamics, gravitational forces vary with the inverse square of the distance between celestial objects [4,26]. Similarly, variable-mass systems such as the time-dependent mass pendulum analyzed by Baleanu et al. [3], demonstrate how dynamic behavior is influenced by temporal changes in mass. In living organisms, muscle forces vary as a function of joint kinematics and levels of fatigue. These differing examples form the basis for including force variation in dynamic analysis.

2020 *Mathematics Subject Classification:* 53A04, 53A55, 53A17.
Submitted March 02, 2026. Published July 03, 2026.

The physical quantity referred to as yank, time derivative of force, is crucial for the understanding of transient mechanical response, particularly in systems that experience sudden change or high operational responsiveness. While firmly established on the basis of biomechanical research [16], yank has been comparatively little practiced in differential geometry, especially in applications to Euclidean 3-space. The research in this study seeks to link these two areas through variable-mass object motion using the Darboux frame mathematical model, considering geodesic curvature, normal curvature and geodesic torsion properties [7,23].

In the field of differential geometry and kinematics, the study of higher-order derivatives of motion such as acceleration, jerk, and snap has evolved significantly over the years, particularly in their geometric interpretation through space curves and frames. Previous studies have explored these concepts extensively. For instance, Siacci introduced the acceleration vector in 1879 [24], while Casey revisited Siacci's resolution of the acceleration vector for space curves, providing a modern mathematical treatment of classical mechanical concepts [5]. In 2012, Doğan and Yaylı explored tubes with Darboux frames, extending the use of this frame in curve and surface analysis [8]. Further advancements were made by Özen et al. (2017), who reformulated Siacci's theorem according to the Darboux frame [20], and by Şentürk and Yüce (2019), who examined the evolute offsets of ruled surfaces using the same frame [22]. In 2019, Özen et al. introduced an alternative approach to jerk in motion along a space curve [18], followed by Özen (2020), who adapted Siacci's theorem to Frenet curves in Minkowski 3-space [17], and by Özen et al. (2020), who studied acceleration and jerk along general space curves [19].

The application of these geometric resolutions expanded to new mechanical and physical interpretations in the following decade. In 2021, Elsayied et al. presented a new visualization of fundamental mechanical elements and concepts through differential geometry [9], while Hamouda et al. offered a detailed resolution of jerk and snap vectors for quasi curves in Euclidean 3-space [15]. In 2023, Tawfiq et al. introduced a new method for resolving jerk and jounce vectors in Euclidean settings [25]. Most recently, in 2024, Elsharkawy et al. extended these ideas to non-lightlike curves in Minkowski 3-space, emphasizing the relativistic implications of higher-order motions [10], and Öztürk investigated the Darboux frame of the pancake curve within Euclidean geometry [21]. Together, these works trace a coherent historical progression from the reinterpretation of classical motion concepts to modern geometric formulations in both Euclidean and Minkowski spaces.

This paper is organized as follows:

- **Section 2**: provides the essential preliminaries on the Frenet and Darboux frames for particles moving along space curves.
- **Section 3**: establishes the theoretical framework, resolving momentum, force, and yank vectors in Frenet and Darboux frames, and extends the analysis to radial decompositions via projections onto osculating and rectifying planes.
- **Section 4**: demonstrates applications of the derived formulations in constant-mass and variable-mass systems, focusing on slant helix and regular curve trajectories.
- **Section 5**: concludes the study by summarizing the principal findings in particle dynamics and differential geometry, and suggesting potential extensions to relativistic and stochastic motion models.

2. Preliminary

Let $\boldsymbol{\alpha}(s)$ be a regular curve in the three-dimensional Euclidean space $\mathbb{E}^3$, equipped with the standard inner product. For any vectors $\mathbf{x} = (x_1, x_2, x_3)$ and $\mathbf{y} = (y_1, y_2, y_3)$, this product is defined by

$$\langle \mathbf{x}, \mathbf{y} \rangle = x_1 y_1 + x_2 y_2 + x_3 y_3.$$

If the curve is parameterized by arc length s, one can associate to each point the Frenet frame $\{\mathbf{T}(s), \mathbf{N}(s), \mathbf{B}(s)\}$, consisting of the tangent, principal normal, and binormal vectors, respectively [6,7, 23]. These vectors are expressed as

$$\mathbf{T}(s) = \boldsymbol{\alpha}'(s), \quad \mathbf{N}(s) = \frac{\boldsymbol{\alpha}''(s)}{\|\boldsymbol{\alpha}''(s)\|}, \quad \mathbf{B}(s) = \mathbf{T}(s) \times \mathbf{N}(s), \tag{2.1}$$

where differentiation is taken with respect to s [11,12].

The variation of this moving frame along the curve is described by the Frenet-Serret relations

$$\begin{pmatrix} \mathbf{T}'(s) \\ \mathbf{N}'(s) \\ \mathbf{B}'(s) \end{pmatrix} = \begin{pmatrix} 0 & \kappa(s) & 0 \\ -\kappa(s) & 0 & \tau(s) \\ 0 & -\tau(s) & 0 \end{pmatrix} \begin{pmatrix} \mathbf{T}(s) \\ \mathbf{N}(s) \\ \mathbf{B}(s) \end{pmatrix}, \tag{2.2}$$

where $\kappa(s)$ and $\tau(s)$ denote, respectively, the curvature and torsion of the curve [2,13] given by

$$\begin{aligned} \kappa(s) &= \|\mathbf{T}'(s)\| = \langle \mathbf{T}'(s), \mathbf{N}(s) \rangle = -\langle \mathbf{N}'(s), \mathbf{T}(s) \rangle, \\ \tau(s) &= \langle \mathbf{N}'(s), \mathbf{B}(s) \rangle = -\langle \mathbf{B}'(s), \mathbf{N}(s) \rangle. \end{aligned} \tag{2.3}$$

Let $\alpha : I \subset \mathbb{R} \to M$ be a unit-speed curve lying on a smooth surface M. Along this curve, one can introduce the Darboux frame $\{\mathbf{T}, \mathbf{S}, \mathbf{n}\}$. Here, $\mathbf{T}$ denotes the unit tangent of α, $\mathbf{n}$ is the unit normal to the surface M restricted to the curve, and $\mathbf{S}$ is defined as $\mathbf{S} = \mathbf{n} \times \mathbf{T}$. Since $\mathbf{T}$ appears in both the Frenet-Serret and Darboux frames, the remaining vectors in each system differ only by a rotation in the normal plane [8]. Hence, the relation between the two frames can be written in matrix form as

$$\begin{pmatrix} \mathbf{T} \\ \mathbf{N} \\ \mathbf{B} \end{pmatrix} = \begin{pmatrix} 1 & 0 & 0 \\ 0 & \cos\theta & \sin\theta \\ 0 & -\sin\theta & \cos\theta \end{pmatrix} \begin{pmatrix} \mathbf{T} \\ \mathbf{S} \\ \mathbf{n} \end{pmatrix}, \tag{2.4}$$

where θ denotes the angle between $\mathbf{S}$ and $\mathbf{N}$, or equivalently between $\mathbf{n}$ and $\mathbf{B}$ [20].

The variation of the Darboux frame along α is described by

$$\begin{pmatrix} \mathbf{T}' \\ \mathbf{S}' \\ \mathbf{n}' \end{pmatrix} = \begin{pmatrix} 0 & k_g & k_n \\ -k_g & 0 & \tau_g \\ -k_n & -\tau_g & 0 \end{pmatrix} \begin{pmatrix} \mathbf{T} \\ \mathbf{S} \\ \mathbf{n} \end{pmatrix}, \tag{2.5}$$

where k_g, k_n, and τ_g represent the geodesic curvature, the normal curvature, and the geodesic torsion of the curve, respectively [21].

These quantities are related to the Frenet invariants κ and τ through the following relations

$$\begin{aligned} k_g(s) &= \kappa(s)\cos\theta, \qquad & \kappa^2(s) &= k_g^2(s) + k_n^2(s), \\ k_n(s) &= \kappa(s)\sin\theta, & \theta &= \arctan\left(\tfrac{k_n}{k_g}\right), \\ \tau_g(s) &= \tau(s) - \theta'(s). \end{aligned} \tag{2.6}$$

Definition 2.1 *The first and second derivatives of the momentum vector are referred to as the force and yank vectors, respectively.*

Notation 1 *[1,14] For a particle moving along the curve C, we denote by π_1 the osculating plane and by π_2 the rectifying plane at each point. Let B and Y be the feet of the perpendiculars from the origin O onto π_1 and π_2, respectively. The position vectors of the particle relative to B and Y are denoted by $\mathbf{r}$ and $\mathbf{r}^*$, with corresponding unit vectors $\mathbf{e}_r$ and $\mathbf{e}_{r^*}$ directed from B and Y toward the particle P.*

3. Variable-Mass Dynamics

In this section, we derive the decomposition of the force and yank vectors for a particle with variable mass moving in a Darboux frame, and further present an alternative formulation of these vectors in terms of the tangential component and two distinct radial components lying in the osculating and rectifying plane.

Theorem 3.1 *Consider a particle P with variable mass m moving along a curve C in three-dimensional Euclidean space $\mathbb{E}^3$, assuming that the components of its momentum vector are never zero. Then, the momentum, force, and yank can be expressed as follows*

$$\boldsymbol{P}(t) = m(t)\boldsymbol{v}(t) = m\dot{s}\,\boldsymbol{T}, \tag{3.1}$$

$$\boldsymbol{F}(t) = (\dot{m}v + m\dot{v})\,\mathbf{T} + m\kappa v^2\,\mathbf{N}, \tag{3.2}$$

$$\boldsymbol{Y}(t) = \left(\ddot{m}v + 2\dot{m}\dot{v} + m\ddot{v} - m\kappa^2 v^3\right)\mathbf{T} + \left(2\dot{m}\kappa v^2 + 3m\kappa v\dot{v} + mv^2\dot{\kappa}\right)\mathbf{N} + \left(m\kappa\tau v^3\right)\mathbf{B}. \tag{3.3}$$

Proof: Let P be a particle of mass m moving on a regular surface M, and let a fixed origin O be chosen in $\mathbb{E}^3$. Denote by $\mathbf{x}(t)$ the position vector of P at time t, and let C be the oriented curve traced by the particle. If the curve is parameterized by arc length s, chosen so that the arc length corresponds to the time variable, then the unit tangent vector of C is

$$\mathbf{T} = \mathbf{x}' = \frac{d\mathbf{x}}{ds}.$$

The velocity vector of P at time t are therefore expressed as

$$\mathbf{v} = \dot{\mathbf{x}} = v\mathbf{T}, \qquad \text{where } v = \dot{s}, \tag{3.4}$$

where a superposed dot indicates differentiation with respect to t.
Consequently, we can deduce the momentum vector using Equation 3.4,

$$\mathbf{P}(t) = m(t)\mathbf{v} = mv\mathbf{T}.$$

From Definition 2.1, the force and yank vectors of the point P in the Frenet frame are expressed in (3.2) and (3.3), respectively. These follow directly from Equations (2.1), (2.2) and (2.3). □

Theorem 3.2 *Let a point particle P of variable mass m move along a curve C in the Euclidean space $\mathbb{E}^3$, assuming that the components of its momentum vector are never zero. Then, the following results hold in Darboux frame*

- *The force vector of the particle P at time t can be expressed as*

$$\mathbf{F}(t) = (\dot{m}v + m\dot{v})\,\mathbf{T} + mv^2 k_g\,\mathbf{S} + mv^2 k_n\,\mathbf{n}. \tag{3.5}$$

- *The yank vector of the particle P at time t can be expressed as*

$$\mathbf{Y}(t) = Y_T\mathbf{T} + Y_g\mathbf{S} + Y_n\mathbf{n}, \tag{3.6}$$

where

$$\begin{aligned}
Y_T =& m\left(\ddot{v} - (k_g^2 + k_n^2)v^3\right) + v\ddot{m} + 2\dot{v}\dot{m}\,,\\
Y_g =& \left(m\left(3v\dot{v}\sqrt{k_g^2+k_n^2} + v^2\frac{d}{dt}\left(\sqrt{k_g^2+k_n^2}\right)\right) + 2v^2\dot{m}\sqrt{k_g^2+k_n^2}\right)\cos\theta -\\
& \left(mv^3(\tau_g + \theta')\sqrt{k_g^2+k_n^2}\right)\sin\theta,\\
Y_n =& \left(m\left(3v\dot{v}\sqrt{k_g^2+k_n^2} + v^2\frac{d}{dt}\left(\sqrt{k_g^2+k_n^2}\right)\right) + 2v^2\dot{m}\sqrt{k_g^2+k_n^2}\right)\sin\theta +\\
& \left(mv^3(\tau_g + \theta')\sqrt{k_g^2+k_n^2}\right)\cos\theta.
\end{aligned}$$

Here, Y_T, Y_g andY_n are the tangent, geodesic and normal vectors components of the yank, respectively.

Proof: From Definition 2.1 and Equation (3.1), the force and yank vectors of the point P in the Darboux frame are expressed in (3.5) and (3.6), respectively. These follow directly using Equations (2.4), (2.5), and (2.6). □

3.1. Radial Decomposition Method

The radial decomposition provides an alternative geometric perspective on force and yank vectors by resolving them into components that align with physically meaningful directions in the osculating and rectifying planes. Unlike the Frenet-Darboux basis, which uses intrinsic curve properties, the radial approach employs:

- The **tangential direction T**: aligned with instantaneous motion.
- The **first radial direction $\mathbf{e}_r$**: perpendicular to **T** in the osculating plane π_1, pointing from the center of curvature toward the particle.
- The **second radial direction $\mathbf{e}_{r^*}$**: perpendicular to **T** in the rectifying plane π_2, capturing torsion effects.

This decomposition is particularly useful for analyzing centripetal effects (first radial) and helical motion (second radial) separately, providing direct physical interpretation for curved trajectory dynamics. The distances r and r^* represent the particle's separation from reference points in each plane, making the formulation intuitive for engineering applications.

Theorem 3.3 *Let a point particle P of variable mass m move along a curve C in the Euclidean space $\mathbb{E}^3$, assuming that the components of its momentum vector are never zero. Then, the force, and yank in the direction of the unit tangent, first radial, and second radial vectors in the Darboux frame are as follows:*

- *The force vector of the particle P at time t can be expressed as*

$$\mathbf{F}(t) = \left[m \left(\dot{v} + \frac{qv^2 \sqrt{k_g^2 + k_n^2}}{p} \right) + \dot{m}v \right] \mathbf{T} - \left[\frac{mrv^2 \sqrt{k_g^2 + k_n^2}}{p} \right] \mathbf{e}_r. \tag{3.7}$$

- *The yank vector of the particle P at time t can be expressed as*

$$\mathbf{Y}(t) = Y_{T^*}\mathbf{T} + Y_r \mathbf{e}_r + Y_{r^*}\mathbf{e}_{r^*}, \tag{3.8}$$

where

$$\begin{aligned}
Y_{T^*} =& m\left(\ddot{v} - v^3(k_g^2 + k_n^2) + \frac{q}{p}\left(3v\dot{v}\sqrt{k_g^2 + k_n^2} + v^2 \frac{d}{dt}(\sqrt{k_g^2 + k_n^2}) \right) - (\frac{q}{b})v^3(\tau_g + \theta')\sqrt{k_g^2 + k_n^2} \right) \\
&+ 2\dot{m}\left(\dot{v} + (\frac{q}{p})v^2\sqrt{k_g^2 + k_n^2} \right) + v\ddot{m}, \\
Y_r =& -\frac{r}{p}\left(m\left(3v\dot{v}\sqrt{k_g^2 + k_n^2} + v^2\frac{d}{dt}(\sqrt{k_g^2 + k_n^2}) \right) + 2v^2\dot{m}\sqrt{k_g^2 + k_n^2} \right), \\
Y_{r^*} =& m(\frac{r^*}{b})v^3(\tau_g + \theta')\sqrt{k_g^2 + k_n^2}.
\end{aligned}$$

Here, Y_{T^*}, Y_r andY_{r*} are the tangent, first radial, and second radial vectors components of the yank, respectively.

Proof: Let a particle P traverse an arc-length parameterized $\alpha(s)$ in the Euclidean space $\mathbb{E}^3$. The position vector $\mathbf{x}$ of P can be represented with respect to the Darboux frame as:

$$\mathbf{x} = q\mathbf{T} - p(\cos\theta\,\mathbf{S} + \sin\theta\,\mathbf{n}) + b(-\sin\theta\,\mathbf{S} + \cos\theta\,\mathbf{n}),$$

where

$$q = \langle \mathbf{x}, \mathbf{T} \rangle, \quad p = -\langle \mathbf{x}, \cos\theta\,\mathbf{S} + \sin\theta\,\mathbf{n} \rangle, \quad b = \langle \mathbf{x}, -\sin\theta\,\mathbf{S} + \cos\theta\,\mathbf{n} \rangle. \tag{3.9}$$

The vectors $\mathbf{T}$, $(\cos\theta\,\mathbf{S} + \sin\theta\,\mathbf{n})$, and $(-\sin\theta\,\mathbf{S} + \cos\theta\,\mathbf{n})$ form an orthonormal set.
Based on this, we introduce

$$\mathbf{r} = q\mathbf{T} - p(\cos\theta\,\mathbf{S} + \sin\theta\,\mathbf{n}), \qquad \mathbf{r}^* = q\mathbf{T} + b(-\sin\theta\,\mathbf{S} + \cos\theta\,\mathbf{n}), \tag{3.10}$$

which are contained in the planes π_1 and π_2 associated with α at P, respectively. It then follows that:

$$r^2 = \langle \mathbf{r}, \mathbf{r} \rangle = q^2 + p^2, \qquad (r^*)^2 = \langle \mathbf{r}^*, \mathbf{r}^* \rangle = q^2 + b^2, \tag{3.11}$$

where r and r^* denote the Euclidean norms of $\mathbf{r}$ and $\mathbf{r}^*$, respectively (see Figure 1). Also, we can define the vectors $\mathbf{r}$ and $\mathbf{r}^*$ as:

$$\mathbf{r} = r\mathbf{e}_r, \qquad \mathbf{r}^* = r^*\mathbf{e}_{r^*}.$$

Thus, Equation (3.10) becomes

$$\cos\theta\,\mathbf{S} + \sin\theta\,\mathbf{n} = \frac{1}{p}(q\mathbf{T} - r\mathbf{e}_\mathbf{r}), \qquad -\sin\theta\,\mathbf{S} + \cos\theta\,\mathbf{n} = \frac{1}{b}(-q\mathbf{T} + r^*\mathbf{e}_{r*}). \tag{3.12}$$

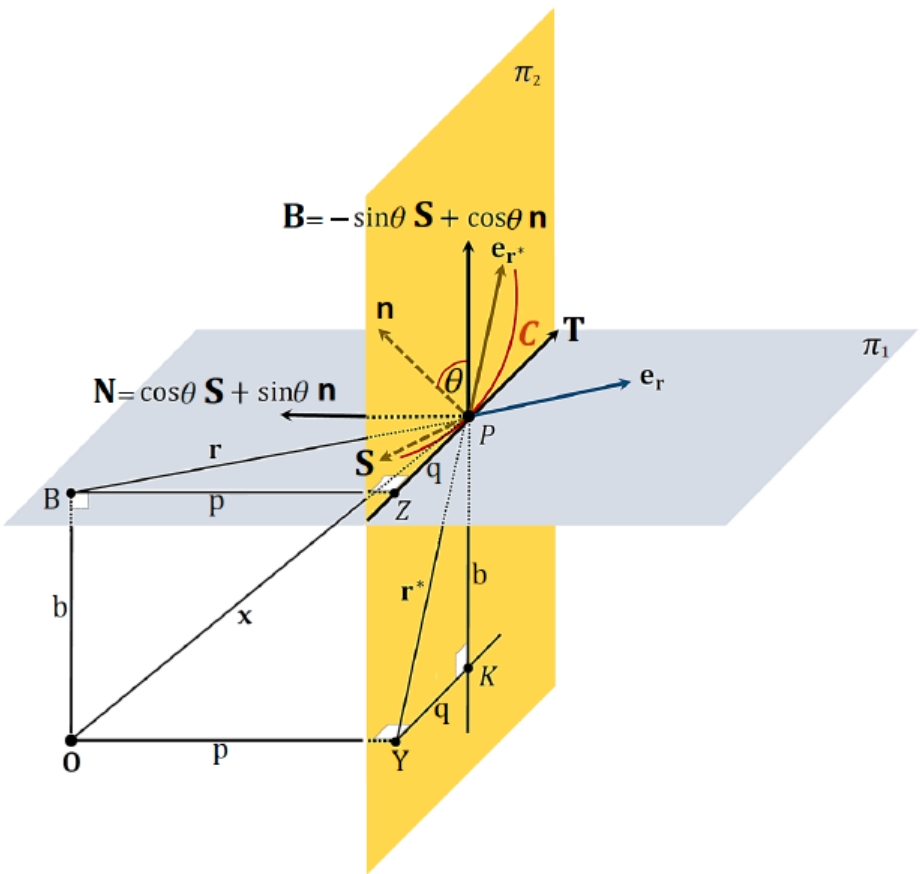

Figure 1: The motion of a particle P along a curve C in Darboux frame.

The force and yank vectors given in (3.5) and (3.6) can therefore be written as

$$\mathbf{F}(t) = (\dot{m}v + m\dot{v})\,\mathbf{T} + m\sqrt{k_g^2 + k_n^2}\,v^2\,(\cos\theta\,\mathbf{S} + \sin\theta\,\mathbf{n}), \tag{3.13}$$

and

$$\begin{aligned}\mathbf{Y}(t) = {} & \left(m(\ddot{v} - (k_g^2 + k_n^2)v^3) + v\ddot{m} + 2\dot{v}\dot{m}\right)\mathbf{T} \\ & + \left(m\left(3v\dot{v}\sqrt{k_g^2 + k_n^2} + v^2\frac{d}{dt}\sqrt{k_g^2 + k_n^2}\right) + 2v^2\dot{m}\sqrt{k_g^2 + k_n^2}\right)(\cos\theta\,\mathbf{S} + \sin\theta\,\mathbf{n}) \\ & + \left(mv^3(\tau_g + \theta'(s))\sqrt{k_g^2 + k_n^2}\right)(-\sin\theta\,\mathbf{S} + \cos\theta\,\mathbf{n}).\end{aligned} \tag{3.14}$$

By substituting (3.12) in (3.13) and (3.14), the force and yank vectors can be expressed as in (3.7) and (3.8), respectively. □

Corollary 3.1 *For the case of variable-mass motion where a rocket expels fuel at a constant rate, the rate of mass change is given by* $\mu = \frac{dm}{dt}$ *with* $\mu < 0$. *The rocket's instantaneous mass is therefore* $m(t) = m_0 + \mu t$. *Under these conditions, the associated force and yank vectors in the Darboux frame can be expressed as follows*

- *The force and yank vector of the particle* P *at time* t *can be expressed as*

$$\mathbf{F}(t) = (\mu v + m\dot{v})\,\mathbf{T} + mv^2 k_g\,\mathbf{S} + mv^2 k_n\,\mathbf{n}, \tag{3.15}$$

$$\mathbf{Y}(t) = Y_T\mathbf{T} + Y_g\mathbf{S} + Y_n\mathbf{n}, \tag{3.16}$$

where

$$\begin{aligned}
Y_T =& m\left(\ddot{v} - (k_g^2 + k_n^2)v^3\right) + 2\dot{v}\mu\,,\\
Y_g =& \left(m\left(3v\dot{v}\sqrt{k_g^2+k_n^2} + v^2\frac{d}{dt}\left(\sqrt{k_g^2+k_n^2}\right)\right) + 2v^2\mu\sqrt{k_g^2+k_n^2}\right)\cos\theta -\\
& \left(mv^3(\tau_g+\theta')\sqrt{k_g^2+k_n^2}\right)\sin\theta,\\
Y_n =& \left(m\left(3v\dot{v}\sqrt{k_g^2+k_n^2} + v^2\frac{d}{dt}\left(\sqrt{k_g^2+k_n^2}\right)\right) + 2v^2\mu\sqrt{k_g^2+k_n^2}\right)\sin\theta +\\
& \left(mv^3(\tau_g+\theta')\sqrt{k_g^2+k_n^2}\right)\cos\theta.
\end{aligned}$$

- *Similarly, the radial decomposition yields:*

$$\mathbf{F}(t) = \left[m\left(\dot{v} + \frac{qv^2\sqrt{k_g^2+k_n^2}}{p}\right) + \mu v\right]\mathbf{T} - \left[\frac{mrv^2\sqrt{k_g^2+k_n^2}}{p}\right]\mathbf{e}_r, \tag{3.17}$$

$$\mathbf{Y}(t) = Y_{T^*}\mathbf{T} + Y_r\mathbf{e}_r + Y_{r^*}\mathbf{e}_{r^*}, \tag{3.18}$$

where

$$\begin{aligned}
Y_{T^*} =& m\left(\ddot{v} - v^3(k_g^2+k_n^2) + \frac{q}{p}\left(3v\dot{v}\sqrt{k_g^2+k_n^2} + v^2\frac{d}{dt}(\sqrt{k_g^2+k_n^2})\right) - (\frac{q}{b})v^3(\tau_g+\theta')\sqrt{k_g^2+k_n^2}\right)\\
&+ 2\mu\left(\dot{v} + (\frac{q}{p})v^2\sqrt{k_g^2+k_n^2}\right),\\
Y_r =& -\frac{r}{p}\left(m\left(3v\dot{v}\sqrt{k_g^2+k_n^2} + v^2\frac{d}{dt}(\sqrt{k_g^2+k_n^2})\right) + 2v^2\mu\sqrt{k_g^2+k_n^2}\right),\\
Y_{r^*} =& m(\frac{r^*}{b})v^3(\tau_g+\theta')\sqrt{k_g^2+k_n^2}.
\end{aligned}$$

Proof: *We substitute* $\dot{m} = \mu$ *and* $\ddot{m} = 0$ *into Theorem (3.1) and (3.2), we complete the proof.* □

Corollary 3.2 *In the case of a particle with constant mass moving along a space curve* C *in* $\mathbb{E}^3$. *The associated force and yank vectors in the Darboux frame can be expressed as follows*

- *The force vector of the particle* P *at time* t *can be expressed as* $\mathbf{F}(t) = m\,\mathbf{a}(t)$, *where* $\mathbf{a}(t)$ *is the acceleration vector*

$$\mathbf{a}(t) = \dot{v}\,\mathbf{T} + v^2 k_g\,\mathbf{S} + v^2 k_n\,\mathbf{n}.$$

Also, the yank vector of the particle P at time t can be expressed as: $\mathbf{Y}(t) = m\,\mathbf{J}(t)$, *where* $\mathbf{J}(t)$ *is the jerk vector*

$$\begin{aligned}\mathbf{J}(t) =&\big(\dddot{v} - (k_g^2+k_n^2)v^3\big)\mathbf{T}\\ &+\Big(\big(3v\dot{v}\sqrt{k_g^2+k_n^2} + v^2\tfrac{d}{dt}\Big(\sqrt{k_g^2+k_n^2}\Big)\big)\cos\theta - v^3(\tau_g+\theta')\sqrt{k_g^2+k_n^2}\sin\theta\Big)\mathbf{S}\\ &+\Big(\big(3v\dot{v}\sqrt{k_g^2+k_n^2} + v^2\tfrac{d}{dt}\Big(\sqrt{k_g^2+k_n^2}\Big)\big)\sin\theta + v^3(\tau_g+\theta')\sqrt{k_g^2+k_n^2}\cos\theta\Big)\mathbf{n}.\end{aligned}$$

- *Similarly, the radial decomposition yields.*
  The force vector of the particle P at time t can be expressed as $\mathbf{F}(t) = m\,\mathbf{a}(t)$, *where* $\mathbf{a}(t)$ *is the acceleration vector*

$$\mathbf{a}(t) = \left(\dot{v} + \frac{qv^2\sqrt{k_g^2+k_n^2}}{p}\right)\mathbf{T} - \left(\frac{rv^2\sqrt{k_g^2+k_n^2}}{p}\right)\mathbf{e}_r.$$

Also, the yank vector of the particle P at time t can be expressed as $\mathbf{Y}(t) = m\,\mathbf{J}(t)$, *where* $\mathbf{J}(t)$ *is the jerk vector*

$$\begin{aligned}\mathbf{J}(t) =&\left(\dddot{v} - v^3(k_g^2+k_n^2) + \frac{q}{p}\Big(3v\dot{v}\sqrt{k_g^2+k_n^2} + v^2\tfrac{d}{dt}\big(\sqrt{k_g^2+k_n^2}\big)\Big) - \frac{q}{b}v^3(\tau_g+\theta')\sqrt{k_g^2+k_n^2}\right)\mathbf{T}\\ &-\frac{r}{p}\Big(3v\dot{v}\sqrt{k_g^2+k_n^2} + v^2\tfrac{d}{dt}\big(\sqrt{k_g^2+k_n^2}\big)\Big)\mathbf{e}_r + \frac{r^*}{b}v^3(\tau_g+\theta')\sqrt{k_g^2+k_n^2}\,\mathbf{e}_{r^*}.\end{aligned}$$

Proof: *We substitute* $\dot{m} = \ddot{m} = 0$ *into Theorem (3.2) and (3.3), we complete the proof.* □

3.2. Comparison: Frenet vs. Darboux Frames

Both the Frenet and Darboux frames provide intrinsic descriptions of particle dynamics, but each has distinct advantages:

Table 1: Force and Yank Components in Frenet vs. Darboux Frames

Component	**Frenet Frame**	**Darboux Frame**
Force:		
Tangential	$\dot{m}v + m\dot{v}$	$\dot{m}v + m\dot{v}$
Normal	$m\kappa v^2$ (principal normal)	mv^2k_g (geodesic)
Binormal	0	mv^2k_n (normal to surface)
Yank:		
Tangential	$\ddot{m}v + 2\dot{m}\dot{v} + m\ddot{v} - m\kappa^2v^3$	$\ddot{m}v + 2\dot{m}\dot{v} + m\ddot{v} - m(k_g^2+k_n^2)v^3$
Normal/Geodesic	$2\dot{m}\kappa v^2 + 3m\kappa v\dot{v} + mv^2\dot{\kappa}$	$(...)cos\theta - (...)sin\theta$
Binormal/Surface	$m\kappa\tau v^3$	$(...)sin\theta + (...)cos\theta$

When to use Frenet frame:

- For free space curves without reference surface (e.g., spacecraft trajectories)
- When curvature κ and torsion τ are primary geometric invariants
- For theoretical analysis where surface embedding is not relevant

When to use Darboux frame:

- For constrained motion on surfaces (e.g., vehicles on terrain, particles on manifolds)
- When geodesic properties (k_g, τ_g) have physical meaning
- For problems where surface-normal forces are distinct from in-surface dynamics
- In numerical simulations where $\theta(s)$ can be computed from surface geometry

Key insight: The Darboux frame decomposes normal acceleration into geodesic curvature k_g (bending within the surface) and normal curvature k_n (bending away from the surface), providing richer information for constrained systems. The relation $\kappa^2 = k_g^2 + k_n^2$ shows that Frenet curvature combines these effects.

3.3. Physical Interpretation of Yank Components

The yank vector components reveal distinct physical phenomena in variable-mass dynamics:

Tangential component Y_T (or Y_{T^*}): This captures the rate of change of force along the direction of motion. It includes:

- Contributions from mass variation rate changes ($\dddot{m}$)
- Acceleration changes ($\ddot{v}$)
- Curvature-induced effects that oppose motion ($-v^3(k_g^2 + k_n^2)$)

In rocket propulsion, Y_T describes how thrust evolves during fuel burn, critical for trajectory optimization.

Geodesic component Y_g: This measures force rate change tangent to the surface, perpendicular to the trajectory. It arises from:

- Changes in geodesic curvature as the path bends within the surface
- Mass flow effects ($\dot{m}$) acting perpendicular to velocity

In biomechanics, Y_g relates to lateral force development during curved motion, such as in running or skating turns.

Normal component Y_n: This represents force rate change perpendicular to the surface, capturing:

- Normal curvature variations
- Surface-relative dynamics

Second radial component Y_{r^*}: This uniquely captures torsion effects ($\tau_g + \theta'$), describing how force changes in the direction perpendicular to both motion and the osculating plane. In helical trajectories (e.g., spiral rocket ascent), Y_{r^*} quantifies the twisting rate of applied forces.

3.4. Significance of Yank in Variable-Mass Systems

Yank analysis is essential in variable-mass dynamics for several reasons:

Rocketry and Propulsion: During launch, rockets experience rapid mass loss ($\dot{m} < 0$) and thrust variations. The yank vector determines:

- Structural loading rates on the vehicle frame
- Control system response requirements (as rapid force changes demand faster actuator responses)
- Trajectory stability, since high yank indicates aggressive maneuvers

Biomechanics: In human and animal locomotion, yank reflects neuromuscular control quality [16]:

- Smooth yank profiles indicate coordinated muscle activation
- High-frequency yank oscillations suggest instability or fatigue

- Injury risk correlates with peak yank magnitudes during impact

Engineering Design: Systems subjected to variable forces require yank-aware design:

- Vibration isolation systems must account for force rate changes
- Robotic manipulators with varying payloads need yank limits to prevent mechanical shock
- Astrodynamics missions with continuous thrust require yank analysis for fuel optimization

The differential-geometric formulation presented here enables precise yank calculation from trajectory geometry alone, facilitating these applications.

4. Computational and Illustrative Examples

In this section, illustrative examples are provided to demonstrate the obtained results.

Example 4.1 *Consider a particle P with variable mass moving along a slant helix in $\mathbb{E}^3$, see Figure (2). The position vector $\mathbf{x}$ of P is given as*

$$\mathbf{x} = \alpha(t) = \left(\frac{1}{6}\sin t + \frac{2}{3}\sin\frac{t}{2},\ \frac{1}{6}\cos t + \frac{2}{3}\cos\frac{t}{2},\ \frac{4\sqrt{2}}{3}\cos\frac{t}{4}\right).$$

The speed of P is

$$v = \frac{ds}{dt} = \frac{1}{2}.$$

Thus, we have

$$s = s(t) = \frac{t}{2},$$

and

$$\dot{v} = \ddot{v} = 0.$$

It is easy to find that the curve can be reparameterized by the arc-length function as

$$\alpha(s) = \left(\frac{1}{6}\sin 2s + \frac{2}{3}\sin s,\ \frac{1}{6}\cos 2s + \frac{2}{3}\cos s,\ \frac{4\sqrt{2}}{3}\cos\frac{s}{2}\right). \tag{4.1}$$

From (2.1), the Frenet frame for the slant helix is

$$\mathbf{T}(s) = \left(\frac{1}{3}\cos 2s + \frac{2}{3}\cos s,\ -\frac{1}{3}\sin 2s - \frac{2}{3}\sin s,\ -\frac{2\sqrt{2}}{3}\sin\frac{s}{2}\right),$$

$$\mathbf{N}(s) = \left(-\frac{4}{3\sqrt{2}}\sin\tfrac{3s}{2},\ -\frac{4}{3\sqrt{2}}\cos\tfrac{3s}{2},\ -\tfrac{1}{3}\right),$$

$$\mathbf{B}(s) = \left(-\tfrac{1}{3}\sin 2s + \tfrac{2}{3}\sin s,\ -\tfrac{1}{3}\cos 2s + \tfrac{2}{3}\cos s,\ -\frac{4}{3\sqrt{2}}\cos\tfrac{s}{2}\right).$$

Thus, the Frenet-curvatures are

$$\kappa(s) = \sqrt{2}\cos\frac{s}{2}, \qquad \tau(s) = \sqrt{2}\sin\frac{s}{2}.$$

From(2.6), the geodesic curvature, the normal curvature, and the geodesic torsion of the curve are

$$k_g(s) = \sqrt{2}\cos\frac{s}{2}\cos\theta, \qquad k_n(s) = \sqrt{2}\cos\frac{s}{2}\sin\theta, \qquad \tau_g(s) = \sqrt{2}\sin\frac{s}{2} - \theta'(s).$$

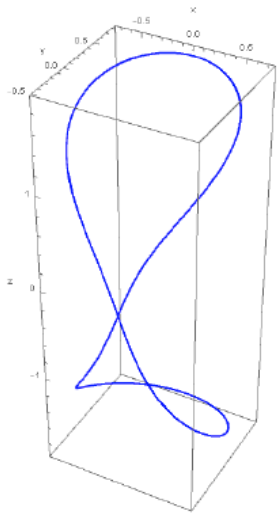

Figure 2: The slant helix curve with view point (1.3, -2.4, 2).

By using (2.4), the Darboux frame vectors for the slant helix are given as follows

$$\mathbf{T}(s) = \left(\frac{1}{3}\cos 2s + \frac{2}{3}\cos s,\ -\frac{1}{3}\sin 2s - \frac{2}{3}\sin s,\ -\frac{2\sqrt{2}}{3}\sin\frac{s}{2}\right),$$

$$\begin{aligned}\mathbf{S}(s) = \Big(&-\tfrac{4}{3\sqrt{2}}\cos\theta\,\sin\tfrac{3s}{2} + \tfrac{1}{3}\sin\theta\,\sin 2s - \tfrac{2}{3}\sin\theta\,\sin s,\\ &-\tfrac{4}{3\sqrt{2}}\cos\theta\,\cos\tfrac{3s}{2} - \tfrac{1}{3}\sin\theta\,\cos 2s - \tfrac{2}{3}\sin\theta\,\cos s,\\ &-\tfrac{1}{3}\cos\theta + \tfrac{4}{3\sqrt{2}}\sin\theta\,\cos\tfrac{s}{2}\Big),\end{aligned}$$

$$\begin{aligned}\mathbf{n}(s) = \Big(&-\tfrac{4}{3\sqrt{2}}\sin\theta\,\sin\tfrac{3s}{2} - \tfrac{1}{3}\cos\theta\,\sin 2s + \tfrac{2}{3}\cos\theta\,\sin s,\\ &-\tfrac{4}{3\sqrt{2}}\sin\theta\,\cos\tfrac{3s}{2} + \tfrac{1}{3}\cos\theta\,\cos 2s + \tfrac{2}{3}\cos\theta\,\cos s,\\ &-\tfrac{1}{3}\sin\theta - \tfrac{4}{3\sqrt{2}}\cos\theta\,\cos\tfrac{s}{2}\Big).\end{aligned}$$

- *By applying Theorem(3.2), we obtain the Force and yank vectors of a variable mass particle P along the Darboux basis*

$$\mathbf{F}(s) = \frac{1}{2}\dot{m}\,\mathbf{T} + \frac{m\sqrt{2}}{4}\cos\frac{s}{2}\cos\theta\,\mathbf{S} + \frac{m\sqrt{2}}{4}\cos\frac{s}{2}\sin\theta\,\mathbf{n},$$

$$\begin{aligned}\mathbf{Y}(s) = &\left[-\frac{m}{4}\cos^2\frac{s}{2} + \frac{1}{2}\ddot{m}\right]\mathbf{T} + \left[\left(-\frac{m\sqrt{2}}{16}\sin\frac{s}{2} + \frac{\dot{m}\sqrt{2}}{2}\cos\frac{s}{2}\right)\cos\theta - \frac{m}{4}\sin s\,\sin\theta\right]\mathbf{S}\\ &+\left[\left(-\frac{m\sqrt{2}}{16}\sin\frac{s}{2} + \frac{\dot{m}\sqrt{2}}{2}\cos\frac{s}{2}\right)\sin\theta + \frac{m}{4}\sin s\,\cos\theta\right]\mathbf{n}.\end{aligned}$$

By means of (3.9), (3.1) and (4.1), we obtain

$$q = -\sin s, \quad p = \sqrt{2}\cos\frac{s}{2}, \quad b = -\frac{1+2\cos s}{2},$$

$$r = \sqrt{2(2-\cos s)}\cos\frac{s}{2}, \quad r^* = \frac{\sqrt{5+4\cos s}}{2}.$$

- *By applying Theorem (3.3), we obtain the Force and yank vectors of a variable mass particle P in radial directions*

$$\mathbf{F}(s) = \left[-\frac{m}{4}\sin s + \frac{1}{2}\dot{m}\right]\mathbf{T} - \frac{m}{4}\sqrt{2(2-\cos s)}\cos\frac{s}{2}\,\mathbf{e}_r,$$

$$\mathbf{Y}(s) = \left[m\left(-\frac{5+5\cos s+2\cos^2 s}{16(1+2\cos s)}\right) - \frac{\dot{m}\sin s}{2} + \frac{1}{2}\ddot{m}\right]\mathbf{T} + \left[\frac{m}{8\sqrt{2}}\sqrt{2-\cos s}\sin\frac{s}{2} - \frac{\dot{m}}{\sqrt{2}}\sqrt{2-\cos s}\cos\frac{s}{2}\right]\mathbf{e}_r - \left[\frac{m\sin s\sqrt{5+4\cos s}}{8(1+2\cos s)}\right]\mathbf{e}_{r^*}.$$

- *By applying Corollary (3.2), we obtain the force and yank vectors for a constant-mass particle*

$$\mathbf{F}(s) = m\left(\frac{\sqrt{2}}{4}\cos\frac{s}{2}\cos\theta\,\mathbf{S} + \frac{\sqrt{2}}{4}\cos\frac{s}{2}\sin\theta\,\mathbf{n}\right),$$

$$\mathbf{Y}(s) = m\Big(-\tfrac{1}{4}\cos^2\left(\tfrac{s}{2}\right)\mathbf{T} + \left(-\tfrac{\sqrt{2}}{16}\sin\left(\tfrac{s}{2}\right)\cos\theta - \tfrac{1}{4}\sin s\,\sin\theta\right)\mathbf{S} + \left(-\tfrac{\sqrt{2}}{16}\sin\left(\tfrac{s}{2}\right)\sin\theta + \tfrac{1}{4}\sin s\,\cos\theta\right)\mathbf{n}\Big).$$

Similarly, the radial decomposition yield,

$$\mathbf{F}(s) = m\left(-\frac{1}{4}\sin s\,\mathbf{T} - \frac{1}{4}\sqrt{2(2-\cos s)}\cos\frac{s}{2}\,\mathbf{e}_r\right),$$

$$\mathbf{Y}(s) = m\left[\left(-\frac{5+5\cos s+2\cos^2 s}{16(1+2\cos s)}\right)\mathbf{T} + \left(\frac{\sqrt{2-\cos s}}{8\sqrt{2}}\sin\frac{s}{2}\right)\mathbf{e}_r - \left(\frac{\sin s\sqrt{5+4\cos s}}{8(1+2\cos s)}\right)\mathbf{e}_{r^*}\right].$$

Example 4.2 *Consider a particle P with variable mass moving along a regular curve in $\mathbb{E}^3$, see Figure (3). The position vector $\mathbf{x}$ of P is given as*

$$\mathbf{x} = \alpha(t) = \left(\frac{3}{2}\cos(t) + \frac{1}{6}\cos(3t), \frac{3}{2}\sin(t) + \frac{1}{6}\sin(3t), \sqrt{3}\cos(t)\right).$$

The speed of P is

$$v = \frac{ds}{dt} = 2.$$

Thus, we have

$$s = s(t) = 2t,$$

and

$$\dot{v} = \ddot{v} = 0.$$

It is easy to find that the curve can be reparameterized by the arc-length function as

$$\alpha(s) = \left(\frac{3}{2}\cos\left(\frac{s}{2}\right) + \frac{1}{6}\cos\left(\frac{3s}{2}\right), \frac{3}{2}\sin\left(\frac{s}{2}\right) + \frac{1}{6}\sin\left(\frac{3s}{2}\right), \sqrt{3}\cos\left(\frac{s}{2}\right)\right). \tag{4.2}$$

From (2.1), the Frenet frame for the regular curve is

$$\mathbf{T}(s) = \left(-\frac{3}{2}\sin\frac{s}{2} + \sin^3\frac{s}{2}, \cos^3\frac{s}{2}, -\frac{\sqrt{3}}{2}\sin\frac{s}{2}\right),$$

$$\mathbf{N}(s) = \left(-\frac{\sqrt{3}}{2}\cos s,\ -\frac{\sqrt{3}}{2}\sin s,\ -\frac{1}{2}\right),$$

$$\mathbf{B}(s) = \left(-\frac{1}{2}\cos\frac{s}{2}\left(1+2\sin^2\frac{s}{2}\right),\ -\sin^3\frac{s}{2},\ \frac{\sqrt{3}}{2}\cos\frac{s}{2}\right).$$

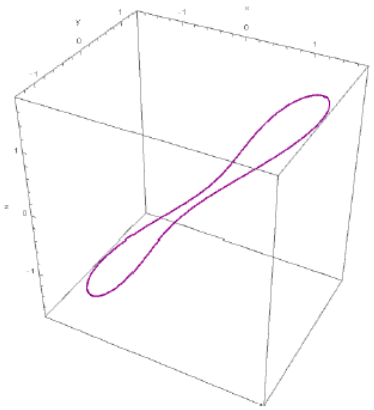

Figure 3: The regular curve with view point (1.3, -2.4, 2).

Thus, the Frenet-curvatures are

$$\kappa(s) = \frac{\sqrt{3}}{2}\cos\frac{s}{2}, \qquad \tau(s) = -\frac{\sqrt{3}}{2}\sin\frac{s}{2}.$$

From(2.6), the geodesic curvature, the normal curvature, and the geodesic torsion of the curve are

$$k_g(s) = \frac{\sqrt{3}}{2}\cos\frac{s}{2}\cos\theta, \qquad k_n(s) = \frac{\sqrt{3}}{2}\cos\frac{s}{2}\sin\theta, \qquad \tau_g(s) = -\frac{\sqrt{3}}{2}\sin\frac{s}{2} - \theta'(s).$$

By using (2.4), the Darboux frame vectors for the regular curve are given as follows

$$\mathbf{T}(s) = \left(-\frac{3}{2}\sin\frac{s}{2} + \sin^3\frac{s}{2},\ \cos^3\frac{s}{2},\ -\frac{\sqrt{3}}{2}\sin\frac{s}{2}\right),$$

$$\begin{aligned}\mathbf{S}(s) = \Big(&-\frac{\sqrt{3}}{2}\cos\theta\cos s + \frac{1}{2}\sin\theta\cos\frac{s}{2}(1+2\sin^2\frac{s}{2}),\\ &-\frac{\sqrt{3}}{2}\cos\theta\sin s + \sin\theta\sin^3\frac{s}{2},\ -\frac{1}{2}\cos\theta - \frac{\sqrt{3}}{2}\sin\theta\cos\frac{s}{2}\Big),\\ \mathbf{n}(s) = \Big(&-\frac{\sqrt{3}}{2}\sin\theta\cos s - \tfrac{1}{2}\cos\theta\cos\frac{s}{2}(1+2\sin^2\frac{s}{2}),\\ &-\frac{\sqrt{3}}{2}\sin\theta\sin s - \cos\theta\sin^3\frac{s}{2},\ -\frac{1}{2}\sin\theta + \frac{\sqrt{3}}{2}\cos\theta\cos\frac{s}{2}\Big).\end{aligned}$$

- *By applying Theorem(3.2), we obtain the Force and yank vectors of a variable mass particle P along the Darboux basis*

$$\mathbf{F}(t) = 2\dot{m}\,\mathbf{T} + 2\sqrt{3}m\cos t\cos\theta\,\mathbf{S} + 2\sqrt{3}m\cos t\sin\theta\,\mathbf{n},$$

$$\begin{aligned}\mathbf{Y}(t) = &\left(-6m\cos^2 t + 2\ddot{m}\right)\mathbf{T} + \left(-2m\sqrt{3}\sin t\cos\theta + 4\sqrt{3}\dot{m}\cos t\cos\theta + 6m\cos t\sin t\sin\theta\right)\mathbf{S}\\ &+ \left(-2m\sqrt{3}\sin t\sin\theta + 4\sqrt{3}\dot{m}\cos t\sin\theta - 6m\cos t\sin t\cos\theta\right)\mathbf{n}.\end{aligned}$$

By means of (3.9), (3.1) and (4.2), we obtain

$$q = -\sin s, \quad p = \frac{4\sqrt{3}}{3}\cos\frac{s}{2}, \quad b = \cos s - \frac{1}{3},$$

$$r = \sqrt{\frac{11}{3} + \frac{8}{3}\cos s - \cos^2 s}, \qquad r^* = \frac{1}{3}\sqrt{10 - 6\cos s}.$$

- *By applying Theorem (3.3), we obtain the Force and yank vectors of a variable mass particle P in radial directions*

$$\mathbf{F}(t) = \left(-\frac{3m}{2}\sin 2t + 2\dot{m}\right)\mathbf{T} - \frac{3m}{2}\sqrt{\frac{11}{3} + \frac{8}{3}\cos 2t - \cos^2 2t}\quad \mathbf{e}_r,$$

$$\mathbf{Y}(t) = \left(m\left(3 - 9\cos^2 t - \frac{3\sin^2 2t}{\cos 2t - \frac{1}{3}}\right) - 3\dot{m}\sin 2t + 2\ddot{m}\right)\mathbf{T}$$
$$+ \left(\frac{3}{2}\left(m\tan t - 2\dot{m}\right)\sqrt{\frac{11}{3} + \frac{8}{3}\cos 2t - \cos^2 2t}\right)\mathbf{e}_r - \left(\frac{m\,\sin 2t\sqrt{10 - 6\cos 2t}}{\cos 2t - \frac{1}{3}}\right)\mathbf{e}_{r^*}.$$

- *By applying Corollary (3.2), we obtain the force and yank vectors for a constant-mass particle*

$$\mathbf{F}(t) = m\left(2\sqrt{3}\cos t\cos\theta\,\mathbf{S} + 2\sqrt{3}\cos t\sin\theta\,\mathbf{n}\right),$$

$$\mathbf{Y}(t) = m\Big[-6\cos^2 t\,\mathbf{T} + \left(-2\sqrt{3}\sin t\cos\theta + 6\cos t\sin t\sin\theta\right)\mathbf{S}$$
$$+ \left(-2\sqrt{3}\sin t\sin\theta - 6\cos t\sin t\cos\theta\right)\mathbf{n}\Big].$$

Similarly, the radial decomposition yield,

$$\mathbf{F}(t) = m\left[-\frac{3}{2}\sin 2t\,\mathbf{T} - \frac{3}{2}\sqrt{\frac{11}{3} + \frac{8}{3}\cos 2t - \cos^2 2t}\,\mathbf{e}_r\right],$$

$$\mathbf{Y}(t) = m\left[\left(3 - 9\cos^2 t - \frac{3\sin^2 2t}{\cos 2t - \frac{1}{3}}\right)\mathbf{T} + \left(\frac{3}{2}\tan t\sqrt{\frac{11}{3} + \frac{8}{3}\cos 2t - \cos^2 2t}\right)\mathbf{e}_r\right.$$
$$\left. - \left(\frac{\sin 2t\sqrt{10 - 6\cos 2t}}{\cos 2t - \frac{1}{3}}\right)\mathbf{e}_{r^*}\right].$$

Example 4.3 ***Rocket Ascent with Linear Mass Decrease***

Consider a rocket following a vertical launch trajectory with a subsequent pitch-over maneuver, modeled as a space curve with:

$$\mathbf{x} = \alpha(t) = \left(R\sin\phi(t),\ 0,\ R(1 - \cos\phi(t))\right),$$

where $\phi(t) = \omega t$ represents pitch angle (ω = pitch rate), and $R = 1000$ m is the characteristic radius. This describes motion in a vertical plane from $t = 0$ (vertical) to $t = \pi/(2\omega)$ (horizontal).

The rocket has:

- *Initial mass: $m_0 = 500$ kg*
- *Fuel burn rate: $\mu = -5$ kg/s (constant)*
- *Pitch rate: $\omega = 0.1$ rad/s*

Thus $m(t) = 500 - 5t$ *kg, valid for* $0 \le t \le 15.7$ *s.*

The speed is:

$$v(t) = \frac{ds}{dt} = R\omega = 100 \text{ m/s (constant thrust assumption).}$$

For this circular arc segment, the arc-length parameterization gives:

$$\alpha(s) = \left(R\sin\frac{s}{R},\ 0,\ R\left(1-\cos\frac{s}{R}\right)\right), \quad s = R\omega t.$$

The Frenet frame vectors are:

$$\mathbf{T}(s) = \left(\cos\frac{s}{R},\ 0,\ \sin\frac{s}{R}\right), \quad \mathbf{N}(s) = \left(-\sin\frac{s}{R},\ 0,\ \cos\frac{s}{R}\right), \quad \mathbf{B}(s) = (0,\ 1,\ 0).$$

The curvature and torsion are:

$$\kappa(s) = \frac{1}{R} = 0.001 \text{ m}^{-1}, \quad \tau(s) = 0 \text{ (planar curve).}$$

Force Analysis (Corollary 3.1): *Using Equation (3.15) with* $\dot{v} = 0$*:*

$$\mathbf{F}(t) = \mu v\mathbf{T} + m\kappa v^2\mathbf{N} = -500\mathbf{T} + (500-5t)(100)(0.001)\mathbf{N} = -500\mathbf{T} + (50-0.5t)\mathbf{N}.$$

At $t = 0$ *(vertical launch):* $\mathbf{F}(0) = -500\mathbf{T} + 50\mathbf{N}$ *(N)*
At $t = 10$ *s:* $\mathbf{F}(10) = -500\mathbf{T} + 45\mathbf{N}$ *(N)*
The tangential force is constant (mass loss effect), while the normal force decreases as mass depletes.
Yank Analysis: *From Corollary 3.1, with* $\ddot{v} = 0$, $\dot{\kappa} = 0$, $\tau = 0$*:*

$$Y_T = -m\kappa^2 v^3 = -(500-5t)(0.001)^2(100)^3 = -(0.5-0.005t) \text{ N/s},$$

$$Y_N = 2v^2\mu\kappa = 2(100)^2(-5)(0.001) = -100 \text{ N/s},$$

$$Y_B = 0 \text{ (no torsion).}$$

Physical Interpretation:

- $Y_T < 0$*: Tangential force decreases due to curvature-velocity coupling*
- $Y_N = -100$ *N/s (constant): Normal force decreases linearly with mass loss*
- *At* $t = 10$ *s,* $Y_T = -0.45$ *N/s while* Y_N *dominates*

This shows that in variable-mass curved flight, yank perpendicular to the trajectory (here Y_N*) often dominates, affecting structural loads and control system design. The constant* Y_N *indicates predictable lateral loading rates, favorable for autopilot design.*

Radial Decomposition: *Using Theorem 3.3 formulation, with* $q = R\sin(s/R)$, $p = R$, $b = 0$ *(osculating circle in plane):*

$$\mathbf{F}(t) = \left[-500 + (50-0.5t)\sin(\omega t)\right]\mathbf{T} - (50-0.5t)\cos(\omega t)\mathbf{e}_r.$$

The radial component $F_r = -(50-0.5t)\cos(\omega t)$ *oscillates with pitch angle, reaching maximum at* $t = 0$ *(vertical,* $F_r = -50$ *N) and zero at horizontal (*$t = \pi/(2\omega)$, $F_r = 0$*).*

This example demonstrates how yank analysis informs:

1. *Structural fatigue:* Y_N *determines cyclic loading rates*
2. *Thrust vectoring requirements:* Y_T *evolution guides throttle control*
3. *Mission planning: Constant* Y_N *simplifies trajectory optimization*

5. Conclusion

This study has established a unified differential-geometric framework for analyzing particle dynamics along space curves, successfully bridging classical mechanics and differential geometry through the intrinsic formulation of momentum, force, and the higher-order derivative yank. By using the Frenet and Darboux frames, we have resolved these dynamic vectors into their radial forms, extending Siacci's classical theorem to provide new perspectives on transient dynamics in both constant and variable-mass systems. The application of this model to specific trajectories verifies its applicability and demonstrates that the differential invariants of the moving frames offer a precise and efficient method of describing force evolution. The work thereby establishes a foundational platform for subsequent research into relativistic motion, stochastic dynamics on random curves, and the study of higher-order derivatives in a generalized geometric framework.

Acknowledgments

We thank the referees for their valuable suggestions and comments that helped improve this manuscript.

References

1. Alghamdi, F. and Elsharkawy, A. (2025). *Fourth-Order Kinematic Analysis: Advanced Decomposition Methods for Particle Motion in Modified Orthogonal Frame*. PLoS ONE, 20(12), e0337900. https://doi.org/10.1371/journal.pone.0337900
2. Baizeed, H., Elsharkawy, A., Cesarano, C. and Ramadan, A. A. (2025). *Smarandache Curves for the Integral Curves with the Quasi Frame in Euclidean 3-Space*. Azerb. J. Math., 15(2), 219–239. https://doi.org/10.59849/2218-6816.2025.2.219
3. Baleanu, D., Jajarmi, A., Defterli, O., Wannan, R., Sajjadi, S. S., and Asad, J. H. (2024). *Fractional investigation of time-dependent mass pendulum*. J. Low Freq. Noise Vib. Act. Control, 43(1), 196–207. https://doi.org/10.1177/14613484231187439
4. Brown, R. G. (2013). *Introductory Physics I: Elementary Mechanics*. USA, Durham, NC: 27708-0305.
5. Casey, J. A. (2011). *Siacci's Resolution of the Acceleration Vector for a Space Curve*. Meccanica, 46(2), 471–476. https://doi.org/10.1007/s11012-010-9296-x
6. Cesarano, C., Elsharkawy, A. and Baizeed, H. (2025). *Construction and Analysis of Smarandache Curves for Integral Binormal Curves in Euclidean 3-Space*. Univ. J. Math. Appl., 8(3), 149–157. https://doi.org/10.32323/ujma.1739984
7. do Carmo, M. P. (2016). *Differential Geometry of Curves and Surfaces*. Revised and updated second edition. Courier Dover Publications.
8. Doğan, F., and Yaylı, Y. (2012). *Tubes with Darboux Frame*. Int. J. Contemp. Math. Sci., 7(16), 751–758.
9. Elsayied, H., Magdi, A., and Elsharkawy, A. (2021). *A New Visualization of Fundamental Mechanical Elements and Concepts According to Differential Geometry*. Rev. Educ., 392, 40–51.
10. Elsharkawy, A., Cesarano, C., and Alhazmi, H. (2024). *On the jerk and snap in motion along non-lightlike curves in Minkowski 3-space*. Math. Methods Appl. Sci., 47(12), 10280–10292. https://doi.org/10.1002/mma.10121
11. Elsharkawy, A., Elsayied, H., Desouky, M., Cesarano, C. and Gasymov, A. (2026). *A Geometric Study of Ruled Surfaces Generated by Frenet Vectors via N-Pedal Curves in E^3*. Azerb. J. Math., 16(1), 3–15. https://doi.org/10.59849/2218-6816.2026.1.3
12. Elsharkawy, A. and Elsharkawy, N. (2025). *Bertrand and Mannheim Curves of Normal-Integral and Binormal-Integral Curves in Euclidean 3-Space*. Bull. Math. Anal. Appl., 17(4). https://doi.org/10.54671/BMAA-2025-4-5
13. Elsharkawy, A., Hamdani, H., Cesarano, C. and Elsharkawy, N. (2025). *Geometric Properties of Smarandache Ruled Surfaces Generated by Integral Binormal Curves in Euclidean 3-Space*. Partial Differ. Equ. Appl. Math., 101298. https://doi.org/10.1016/j.padiff.2025.101298
14. Elshenhab, A. M., Moaaz, O., Dassios, I. and Elsharkawy, A. (2022). *Motion along a Space Curve with a Quasi-Frame in Euclidean 3-Space: Acceleration and Jerk*. Symmetry, 14(8), 1610. https://doi.org/10.3390/sym14081610
15. Hamouda, E., Cesarano, C., Askar, S., and Elsharkawy, A. (2021). *Resolutions of the jerk and snap vectors for a quasi curve in Euclidean 3-space*. Mathematics, 9(23). https://doi.org/10.3390/math9233128
16. Lin, D. C., McGowan, C. P., Blum, K. P., and Ting, L. H. (2019). *Yank: The time derivative of force is an important biomechanical variable in sensorimotor systems*. J. Exp. Biol., 222(18). https://doi.org/10.1242/jeb.180414
17. Özen, K. E. (2020). *Siacci's Theorem for Frenet Curves in Minkowski 3-Space*. Math. Sci. Appl. E-Notes, 8(1), 159–167. https://doi.org/10.36753/mathenot.693053

18. Özen, K. E., Dündar, F. S., and Tosun, M. (2019). *An alternative approach to jerk in motion along a space curve with applications*. J. Theor. Appl. Mech. (Poland), 57(2), 435–444. https://doi.org/10.15632/jtam-pl/104595

19. Özen, K. E., Güner, M., and Tosun, M. (2020). *A Note on the Acceleration and Jerk in Motion along a Space Curve*. An. Ştiinţ. Univ. "Ovidius" Constanţa, Ser. Mat., 28(1), 151–164. https://doi.org/10.2478/auom-2020-0011

20. Özen, K. E., Tosun, M., and Akyiğit, M. (2017). *Siacci's Theorem According to Darboux Frame*. An. Ştiinţ. Univ. "Ovidius" Constanţa, Ser. Mat., 25(3), 155–165. https://doi.org/10.1515/auom-2017-0042

21. Öztürk, E. (2024). *Darboux Frame of Pancake Curve in Euclidean 3-Space*. Cumhuriyet Sci. J., 45(3), 571–577. https://doi.org/10.17776/csj.1444015

22. Şentürk, G. Y., and Yüce, S. (2019). *On the Evolute Offsets of Ruled Surfaces Using the Darboux Frame*. Commun. Fac. Sci. Univ. Ankara Ser. A1 Math. Stat., 68(2), 1256–1264. https://doi.org/10.31801/cfsuasmas.516604

23. Shifrin, T. (2015). *Differential Geometry: A First Course in Curves and Surfaces*. University of Georgia.

24. Siacci, F. (1879). *Moto per una linea gobba*. Atti R Accad Sci Torino 14: 750-760.

25. Tawfiq, A. M., Cesarano, C., and Elsharkawy, A. (2023). *A new method for resolving the jerk and jounce vectors in Euclidean 3-space*. Math. Methods Appl. Sci., 46(8), 8779–8792. https://doi.org/10.1002/mma.9016

26. Tipler, P. A., and Mosca, G. (2007). *Physics for Scientists and Engineers*. Macmillan.

27. Wolny, J., and Strzałka, R. (2019). *Momentum in the dynamics of variable-mass systems: Classical and relativistic case*. Acta Phys. Pol. A, 135(3), 475–479. https://doi.org/10.12693/APhysPolA.135.475

[1] *Department of Mathematics, Faculty of Science, Tanta University, Tanta, Egypt.*

[2] *Mathematics Department, Faculty of Education, Ain-Shams University, Cairo, Egypt.*

[3] *Section of Mathematics, International Telematic University Uninettuno, Roma, Italy.*

E-mail address: ayman_ramadan@science.tanta.edu.eg, hkelsayied1989@yahoo.com, maytham.desouky@edu.asu.edu.eg, c.cesarano@uninettunouniversity.net